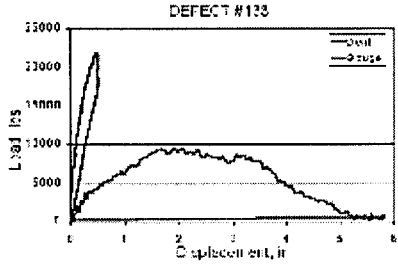
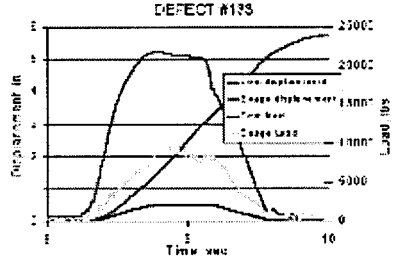
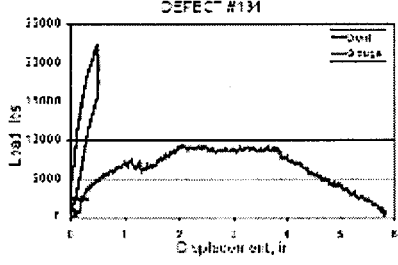
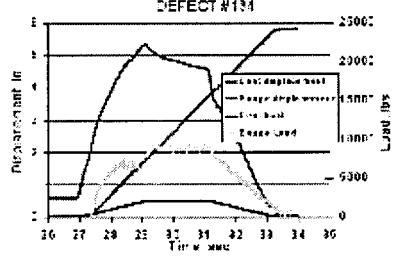
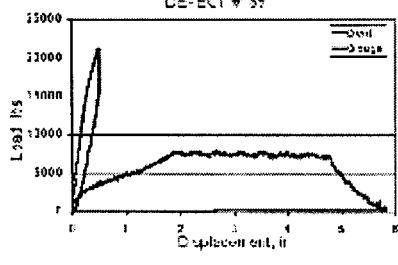
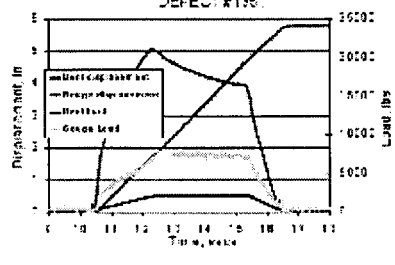
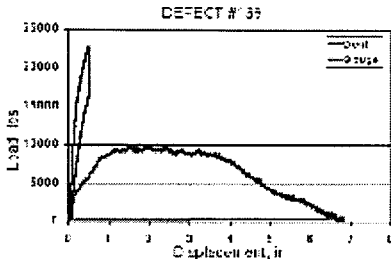
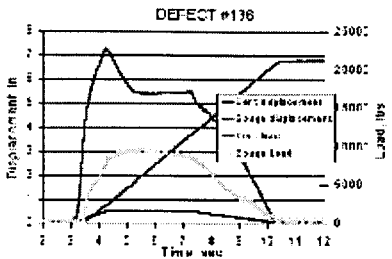
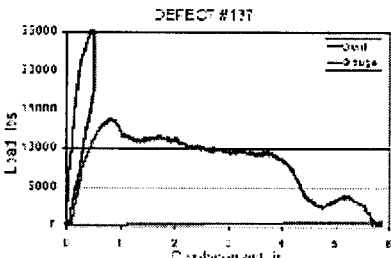
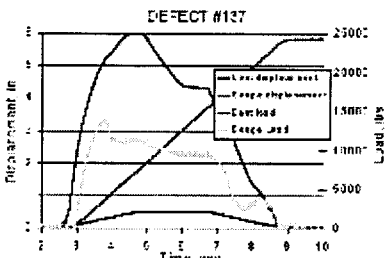
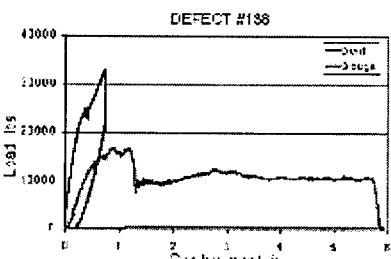
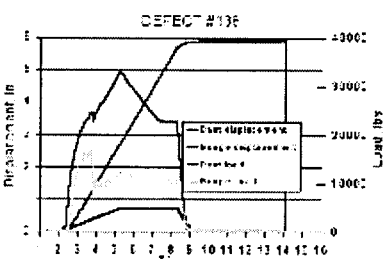
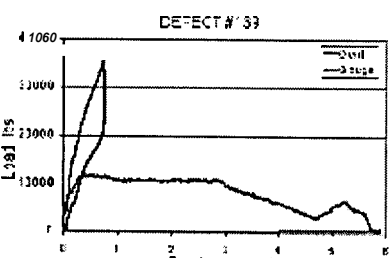
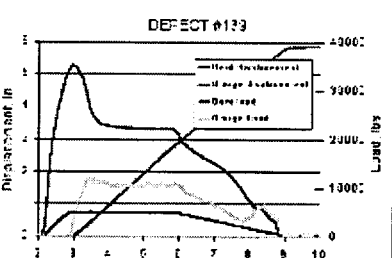


Defect Set 6 - Flow Loop Defects Load-Time-Deflection Plots

This defect set was used in the flow loop. For a layout map of the defects,
click [here](#). For a description of the variables included in this table, see the
legend at the bottom of this page.

#	Load Disp Link	LoadTime Link	D	L	FB	RI	RO	IW	IL	P	S
133			2	6	2	2	2	1	1	0.6	F
134			2	6	2	2	2	1	1	0.6	S
135			2	6	3	2	1	1	1	0.6	S

136			2	6	3	1	2	1	1	0.6	S
137			2	6	2	2	2	5%	5%	0.6	S
138			3	6	3	3	0	5%	5%	0.6	S
139			3	6	3	0	3	5%	5%	0.6	S

140			2	4	2	2	0	1	1	0.6	S
141			1	6	3	1	2	1	1	0.3	F
143			1	6	3	1	2	0.5	1	0.6	S
144			1	6	3	1	2	1	1	0.6	S

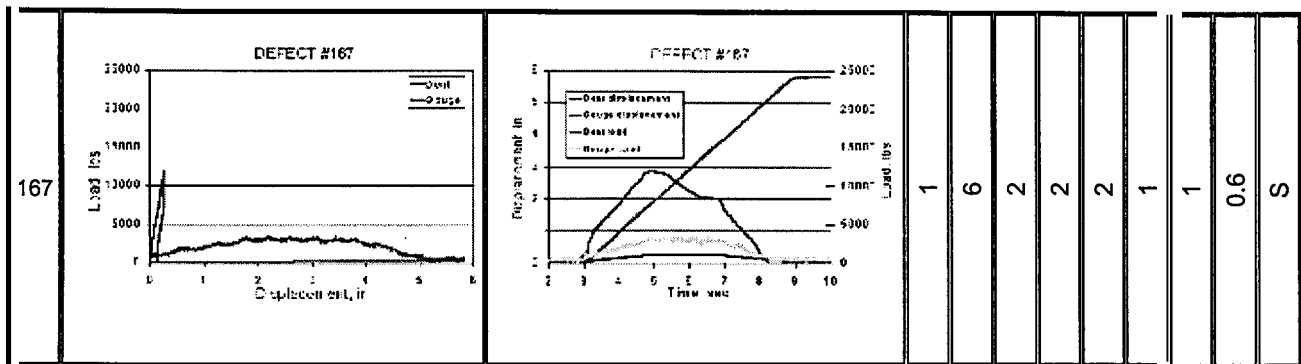
145			2	6	2	2	2	1	1	0.3	S
146			1	6	3	1	2	1	1	0.6	S
148			2	6	2	2	2	1	1	0.6	S
149	NONE	NONE	3	6	0	3	3	5%	5%	0.6	S
150			2	8	2	4	2	1	1	0.6	S

151			1	4	3	1	0	1	1	0.6	S
152			1	6	3	1	2	1	0.5	0.6	S
153			1	6	4	1	1	1	1	0.3	S
154			2	6	3	1	2	1	1	0.3	S

155	<p>DEFECT #155</p>	<p>DEFECT #155</p>	2	6	4	2	0	1	1	0.3	S
156	<p>DEFECT #156</p>	<p>DEFECT #156</p>	2	6	0	2	4	1	1	0.3	S
157	<p>DEFECT #157</p>	<p>DEFECT #157</p>	1	6	4.5	1	0.5	1	1	0.6	S
158	<p>DEFECT #158</p>	<p>DEFECT #158</p>	3	4	1	1.5	1.5	1	1	0.6	S

159	<p>DEFECT #159</p> <p>Load, lbs</p> <p>Displacement, in</p>	<p>DEFECT #159</p> <p>Displacement, in</p> <p>Time, sec</p>	2	6	2	2	2	1	1	0.6	S
160	<p>DEFECT #160</p> <p>Load, lbs</p> <p>Displacement, in</p>	<p>DEFECT #160</p> <p>Displacement, in</p> <p>Time, sec</p>	2	6	2	2	2	1	0.5	0.6	S
161	<p>DEFECT #161</p> <p>Load, lbs</p> <p>Displacement, in</p>	<p>DEFECT #161</p> <p>Displacement, in</p> <p>Time, sec</p>	1	6	3	1	2	0.5	1	0.6	S
162	<p>DEFECT #162</p> <p>Load, lbs</p> <p>Displacement, in</p>	<p>DEFECT #162</p> <p>Displacement, in</p> <p>Time, sec</p>	1	6	2	2	2	1	1	0.6	F

163	NONE		2	6	4	2	0	1	1	0.6	S
164			1	6	4	1	1	1	1	0.6	S
165			2	6	4	1	1	1	1	0.6	S
166			2	6	2	2	2	1	1	0.6	F



Legend:

- e # = Defect# is an arbitrary number identifying each defect
- D = Depth is the dent depth in percent of the diameter.
- e L = Overall Length is the total length of the gouge in inches.
- e FB = Flat Bottom Length is the length of the flat bottom portion of the gouge in inches.
- RI = Ramp In and RO = Ramp Out are the distances on either side of the flat bottom used to ramp the indenter into and out of the pipe (the overall gouge length is the sum of the flat bottom length and the ramp in and ramp out lengths).
- e IW = IndenterWidth and IL = Indenter Length are the footprint dimensions of the indenter in inches; where x% is shown, the indenter was a 4-inch sphere with a sharp protruding cutter that extended x% of the wall thickness.
- e P = Pressure is the internal pipe pressure in percent of specified minimum yield strength.
- e S = Speed refers to the rate of axial movement of the indenter (S is 1 inch per second; F is 5 inches per second).

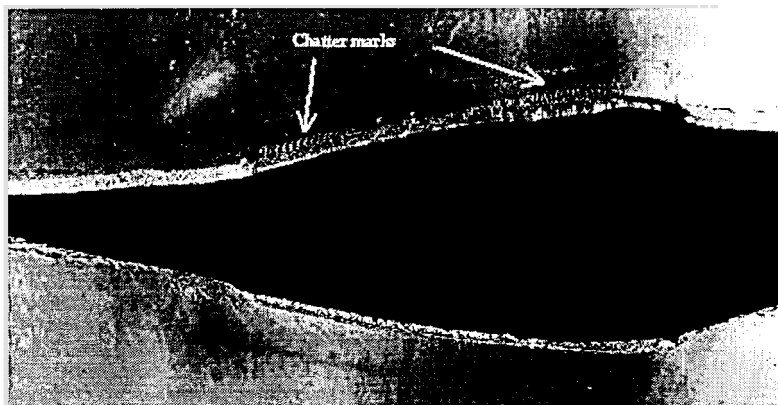
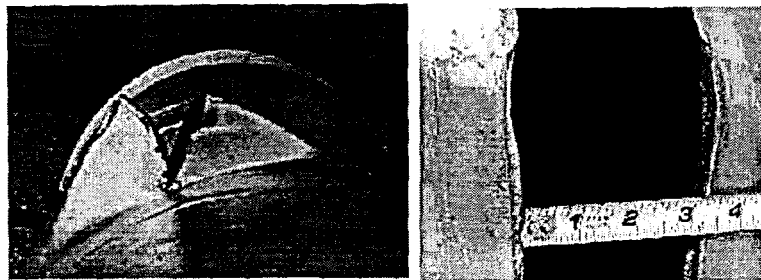
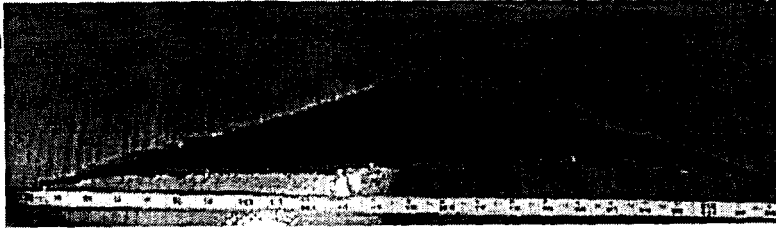
Failure Analyses

Introduction

Analyses were performed on the two defects that failed during repressurization. The analyses indicated the failures had three distinct phases:

- initiation,
- stable tearing, and
- final fracture.

Initiation refers to the formation of a shear-like crack in response to the mechanical damage process. Stable tearing refers to the transition of the shear-like crack to a perpendicular crack and its continued growth by void nucleation growth at the crack tip. Final fracture refers to another transition, in these cases back to a shear crack, and extension of the crack along the axis of the pipe.



The figures at right show one of the failed pipes. The initial mechanical damage is a 6-inch long gouge located in the center one-quarter to one-third of the failure. The gouge includes the "chatter marks" in the lower figure and the region between the chatter marks. The fracture origin is a crack along the gouge and is most clearly seen in the lower photo.

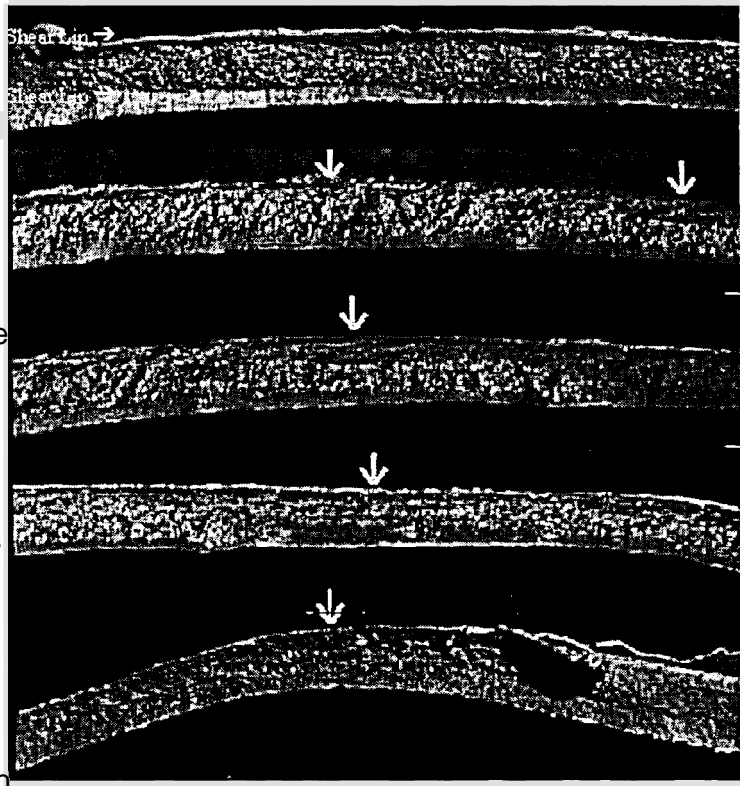
From an inspection perspective, the conditions that lead to initiation of a shear crack are most important. If an initiation crack does not form when creating and rerounding a defect, it is unlikely to form later in typical service. Without an initiation crack, stable crack growth and final fracture cannot occur. Consequently, the conditions that lead to crack initiation were given the strongest emphasis in the failure analyses.

Initiation

In both failures the initiation cracks occurred over the entire length of the fabricated gouge. The figure at right gives a sequence of views, each showing a segment along an initiation site. The top picture begins at the start of the left chatter mark in the above figure, and the bottom picture ends at the end of the right chatter mark. All five photographs when matched end-to-end comprise the entire fabricated gouge.

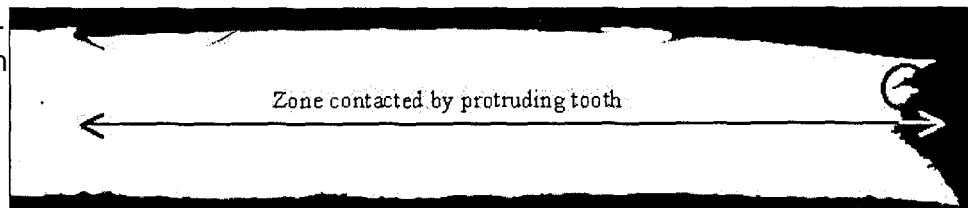
The two failures show shear lips along both the outside and inside diameters (the initial crack and the final fracture). Close examination of the fracture along the outside diameter shows the presence of different textures and colors in

addition to the shear lips. Occasionally, thumbnail-like features are clearly visible without a microscope. For example, in the third view down, an arrow points to an arc-shaped feature that penetrates into one-third of the wall thickness. Other similar, less-well-defined features are indicated by white arrows.



The thumbnail features correspond to local crack initiation sites along the shear lip. A number of shear cracks formed as the pipe rerounds. As the indenter moved down the pipe, the initiation sites merged, leading to the shear lip. Photographs taken at higher magnification and at different angles show many such features along the outside shear lips.

A typical cross-section through the failure is shown at right. This as-polished view



shows the entire cross-section of the gouge and corresponds to a location near the beginning of the damage. (With reference to the top figures, this section lies near the left chatter-mark.) Steel ploughed to the side of the contact area by the protruding tooth

can be seen near the crack at the left edge of the cross-section. The small difference in wall thickness on either side of this crack illustrates that the gouge depth was small.

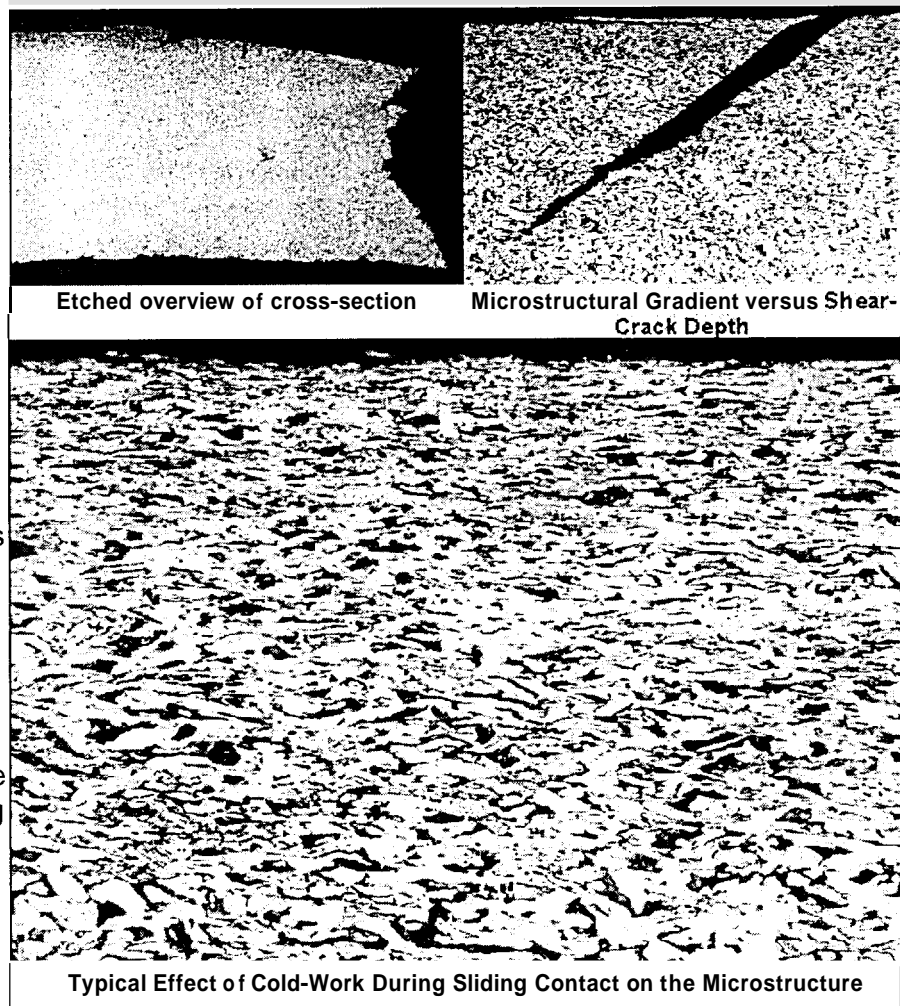
Shear cracking is evident at the failure plane and at the opposite corner of the indenter. Shear cracking is also evident elsewhere across the gouge. At some sites, cracking develops along both shear planes. Hence, multiple initiation sites were formed by the indenter, and these initiation sites are *not* associated only with the stress concentration caused by the sharp edges of the indenter.

The deeper shear cracks also show evidence of opening perpendicular to the crack, indicating the presence of tensile stresses across the crack plane in the hoop direction. These stresses act in addition to the shear stresses, which lie parallel to the direction of shear-crack growth at approximately 45 degrees to the pipe's surface. The significance of the crack opening is discussed below.

An examination of the fractures shows that the shear cracks formed at locations where the microstructure was changed by the mechanical damage.

Presumably, rerounding created conditions that exceeded the local initiation resistance of the material. The figure at right shows the effects of the indenter sliding along the pipe surface. Sliding caused a "pancaking" of the microstructure. (The view shown is along one of the deeper shear cracks.)

The deepest shear cracks penetrate to



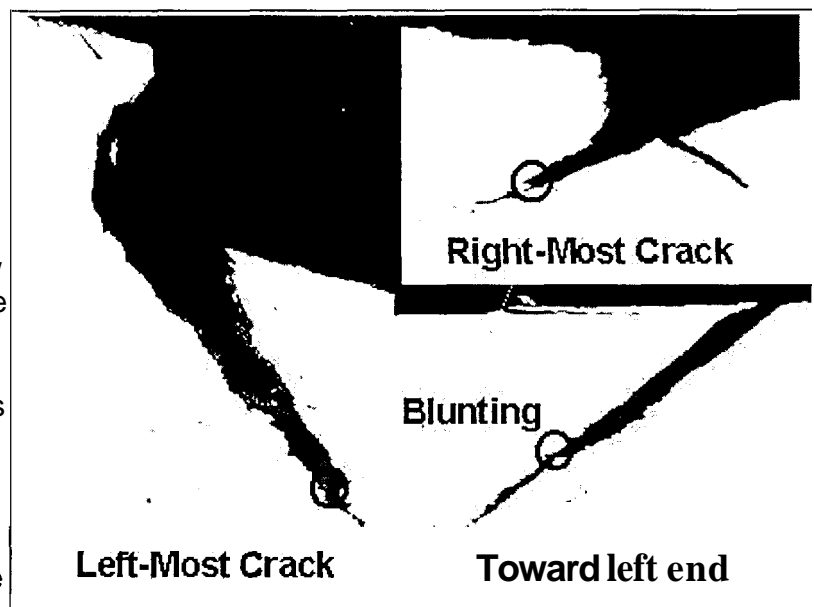
at these locations involves flattening and elongation of the microstructure. There is no evidence of transformation driven by localized heating from contact being quenched by the heat-sink of the unworked steel. (Surface transformations have been seen in some field failure investigations.)

The axial and radial dimensions of the grains below the pancaked layer are roughly equal. That is, there is no preferred orientation of the grains as might be seen in a heavily controlled rolled steel. Near the outside diameter, the grains are extremely long and narrow. Along most of the shear crack, they are elongated to a lesser degree. Near the tip of the crack and below, they return to the original state.

The local strains required to pancake the grains are much larger than those associated with denting or similar geometric changes. They easily reach several tens or hundreds of percent. In addition, the straining is highly anisotropic. These strains and distortions determine the local resistance to crack initiation, and they indicate severe damage.

There is a steep gradient in the hardness of the pancaked grains caused by cold working. Hardness measurements were taken at several locations across and through the pancaked layers. In the undisturbed microstructure, the hardness values ranged from Vickers 200 to 220. Near the surface, some of the hardness values exceeded Vickers 300. At 5 percent depth, the hardness values were typically near Vickers 260, while at 10 percent depth, the values were slightly above the undisturbed hardnesses.

Detailed as-polished view: of a typical cross-section are shown at right. These views confirm that the cracks initiated in response to shear stresses, but they also show that the cracks grew and coalesced under more complex loading. The deeper cracks show regions along their lengths for which the crack opening varies. Such differences in opening correspond to stops and starts in crack growth, due



The largest shear cracks for the two failures extended about 10 percent into the wall thickness, which is the depth of the pancaked region. By the time the cracks reached this depth, void nucleation was occurring around the crack tips. Prior to this time, the cracks initiated and grew intermittently by shear or mixed shear/void nucleation and coalescence. **As** the cracks approached the end of the pancaked region, their growth mechanism transformed from shear to void nucleation and coalescence, and they turned and extended by stable tearing. For this to occur, the loading must have been sufficient to generate large hydrostatic stresses. (At the surface, void nucleation and hydrostatic stresses cannot be generated because the surface stress is zero.)

The hydrostatic stresses needed for void nucleation and growth developed as a result of stretching in the hoop or axial direction. Wall thinning in the hoop direction is evident in the areas where shear cracking eventually turned to through-wall cracking. (Wall thinning local to the failure plane likely occurred as part of the failure, but wall thinning beyond both the failure plane and the gouge likely occurred earlier.) The reduced thickness is associated with stretching while the damage occurred. Initially, this stretching led to strains and stresses in the pancaked region that allowed the shear cracks to form. Then, the stretching generated large tensile stresses, which provided the dominate loading needed to grow the cracks by void nucleation and coalescence.

Thinning remote from the failure plane involved a reduction in wall thickness of up to 15 percent of the nominal thickness. This reduction indicates membrane strains of the same order of magnitude in the vicinity of the gouge and dent. That is, the gouged region was exposed to membrane strains of the order of 15 percent or more. Strains this high are sufficient to initiate cracks in many materials and generate large hydrostatic stresses. In materials with damaged microstructures, such as for these failures, the loading initiated shear cracks and transformed them to stable cracks that continued to grow by void nucleation and coalescence.

Conclusions on the Impact of Initiation Conditions

From an inspection perspective, the most important features associated with mechanical damage are those that relate to the formation of cracks during rerounding. For these failures, the formation of cracks involved (1) the creation of a pancaked and hardened layer and (2) heavy membrane straining.

Stable (Creep) Crack Growth

In both failures, stable crack growth occurred after the initiating shear crack turned perpendicular to the pipe wall. The analyses show that the cracks grew in a stable fashion beyond the shear lip by coalescence of smaller cracks. That is, stable crack growth, like the initial shear cracks, took place at discrete locations, which eventually grew together to form larger cracks. Thus, large thumbnail features on the fracture surface are comprised of smaller cracks, whose crack fronts are also marked with thumbnail-like shapes.

The stable-growth thumbnails can be traced back to the shear crack that initiated and coalesced to form the outside shear lip. Each of the steps in crack opening along the shear cracks and the larger cracks that grew from them are associated with blunting that occurred along the crack tip after each advance of the crack. Surface features on a traverse across the thickness show ductile rupture at all locations, with occasional evidence of a mixed morphology involving some brittle-like tendencies. Dimples are evident almost everywhere, although their shape varies, as expected, from tear-like on the shear planes to more rounded between the shear lips.

High-power scanning electron microscopic examination confirmed that crack advance occurred due to stable tearing involving void nucleation, growth, and coalescence. Stable tearing took place when the driving force for cracking exceeded the material's resistance, and it periodically stopped as loads were redistributed to surrounding regions. So, cracking occurred on a periodic basis between times when the driving force exceeded the material's resistance (due to stretching, an increase in pressure or some other loading) and before the crack blunted and loads were redistributed.

Stable crack growth (creep) is controlled by time at stress rather than the more conventional situation where creep is thermally activated. While the cracking in these failures occurred periodically, it was not fatigue because the cracking mechanism did not involve reversed slip.

Continued creep crack growth required sustained tensile loading, which involved large plastic strains. Given that loads tend to redistribute as plastic flow occurs, sustained tensile loading most likely occurred only during defect formation or subsequent increases in pressure (otherwise an immediate failure would occur). Wall thinning, discussed earlier, is a strong indicator that large, sustained tensile loading can or has occurred. Note that creep crack growth rates are generally independent of initial prestrain because the strain fields at the crack tip easily exceed prestrain levels. So, by the time stable crack growth occurred, the impact of the initial pancaking was lost.

Conclusions on the Impact of Stable Growth

Crack growth beyond the initial shear lip occurred due to creep, void nucleation, growth, and coalescence. The driving force needed for stable crack growth was sustained tensile loading. Wall thinning is a strong indicator that sustained loading can or has occurred.

Final Fracture

Failure in both instances occurred when the overall crack length and depth reached a critical size. The critical size of the crack can be inferred from the shear lip on the inside diameter. In contrast to the shear lip along the outer diameter, the inner shear lip is associated with plastic collapse of the remaining ligament.

The size of the inner shear lip is equal to the size of the plastic zone at the time when

final fracture initiates. Measurements along the fracture indicate the cracks became critical at a depth ranging from 70 to about 85 percent of the thickness.

The size of the shear lip was reasonably large compared to the thickness for both failures. This is consistent with the toughness of the material and with the large strains needed to stably grow the crack. For less tough materials, stable crack growth and final fracture can occur at lower stresses.

Conclusions on the Impact of Final Fracture

Final fracture occurs when the overall crack length and depth reach a critical size. For the samples in these studies, fracture occurred when the cracks were 70 to 85 percent of the wall thickness. Cracks in materials with lower toughness will become unstable at a smaller depth and may be accompanied by less wall thinning.

Summary

The two failures evaluated here occurred as a result of axial cracking that initiated during rerounding in the wake of the tool causing the damage. The cracking developed on a shear plane that formed along the full length of the gouge within the dent. The continuous shear-plane cracks formed by the axial coalescence of a series of individual cracks that initiated during the axial passage of the damage tool.

The shear plane cracking transitioned into a plane normal to the pipe wall, from many individual origins along the deeper areas of the shear plane cracking. These origins grew into the pipe wall as independent cracks. Crack advance occurred in steps, with advance beginning when the increasing pressure caused the crack driving force to exceed the critical level for stable tearing. Cracking ceased when the crack driving force fell below its critical level as loads were redistributed.

After initiation, the mechanism for cracking is stable tearing, which involves void nucleation, growth, and coalescence. This mechanism is fundamentally different from the reversed-slip, striation-forming mechanism involved with the fatigue process. Fracture initiation from the stable-growing crack gave rise to rupture.

From an inspection perspective, the most important features seen in the damage are the presence of a pancaked layer, heavy membrane strains, and associated wall thinning. Detecting and sizing such features will be needed to determine the likelihood of failure and the remaining life of a given mechanical damage defect. For these high toughness materials, wall thinning was appreciable. For lower toughness materials, less wall thinning is likely before a failure occurs.